

# The $G$ -Wishart Weighted Proposal Algorithm: Efficient Posterior Computation for Gaussian Graphical Models

Willem van den Boom\*

Yale-NUS College, National University of Singapore

and

Alexandros Beskos

Department of Statistical Science, University College London

Alan Turing Institute, UK

and

Maria De Iorio

Yong Loo Lin School of Medicine, National University of Singapore

Singapore Institute for Clinical Sciences, A\*STAR

Department of Statistical Science, University College London

## Abstract

Gaussian graphical models can capture complex dependency structures amongst variables. For such models, Bayesian inference is attractive as it provides principled ways to incorporate prior information and to quantify uncertainty through the posterior distribution. However, posterior computation under the conjugate  $G$ -Wishart prior distribution on the precision matrix is expensive for general non-decomposable graphs. We therefore propose a new Markov chain Monte Carlo (MCMC) method named the  $G$ -Wishart weighted proposal algorithm (WWA). WWA's distinctive features include delayed acceptance MCMC, Gibbs updates for the precision matrix and an informed proposal distribution on the graph space that enables embarrassingly parallel computations. Compared to existing approaches, WWA reduces the frequency of the relatively expensive sampling from the  $G$ -Wishart distribution. This results in faster MCMC convergence, improved MCMC mixing and reduced computation time. Numerical studies on simulated and real data show that WWA provides a more efficient tool for posterior inference than competing state-of-the-art MCMC algorithms.

*Keywords:* Exchange algorithm; Hyper inverse Wishart distribution; Locally balanced proposal; Reversible jump MCMC; Scalable Bayesian computations

---

\*Email: willem@yale-nus.edu.sg. This work was supported by the Singapore Ministry of Education Academic Research Fund Tier 2 under Grant MOE2019-T2-2-100.

# 1 Introduction

Gaussian graphical models (GGMs, Dempster, 1972; Lauritzen, 1996) are a powerful tool to investigate conditional independence structure among variables, represented by the nodes of the graph. Graph estimation is often very challenging given the dimensionality of the graph space. In the frequentist literature, different strategies have been proposed to bypass this problem. For example, Friedman et al. (2007) propose the graphical lasso, which involves the estimation of the precision matrix of a multivariate Gaussian vector through penalised likelihood methods. Then, from the estimation of the covariance, the graph is constructed by drawing an edge between variables whose partial correlation is estimated as different from zero. Alternatively, nodewise regression (Zhou et al., 2011) approximates the joint distribution of the variables by considering individual regressions of each variable on the others. This leads to a computationally efficient setup which is also amenable to parallelisation, at the cost of not being founded upon a probabilistically consistent model.

On the other hand, in the Bayesian framework, graph estimation requires the specification of a prior on the space of graphs and, conditionally on the graph, a prior on the precision matrix. Then, posterior inference is performed usually through Markov chain Monte Carlo (MCMC, e.g., Wang and Li, 2012; Hinne et al., 2014) and more recently sequential Monte Carlo (SMC, Tan et al., 2017; van den Boom et al., 2021). However, these methods are often associated with high computational cost and various approaches have been pursued to enable and speed up Bayesian inference in GGMs.

A possible solution is to constrain the analysis to decomposable graphs (e.g., Giudici and Green, 1999; Letac and Massam, 2007; Scott and Carvalho, 2008; Wang, 2010; Bornn and Caron, 2011; Bhadra and Mallick, 2013) or to related subsets of the graph space (Khare et al., 2018) as the associated distributions are tractable. The assumption of decomposability is hard to justify from an applied perspective and increasingly restrictive as the number of nodes increases. In the large data limit where the posterior concentrates, decomposability results in spurious edges which constitute a minimal triangulation of the true graph (Fitch et al., 2014; Niu et al., 2021). In practice, this implies that up to half of the edges in the estimated graph can be spurious, even if the posterior is highly concentrated.

To avoid the assumption of decomposable graphs, Roverato (2002) introduces the  $G$ -Wishart prior distribution for the precision matrix conditional on a graph, which is an extension of the Hyper Inverse Wishart distribution (Dawid and Lauritzen, 1993) employed in the case of decomposable graphs. This allows for more flexibility at the cost of more expensive computations. Given the difficulties to explore the posterior space, stochastic search methods in a Bayesian model have been developed (Jones et al., 2005; Scott and Carvalho, 2008; Lenkoski and Dobra, 2011), which aim to identify graphs with high posterior probability. Nevertheless, MCMC algorithms have received most attention in the literature (e.g., Wang and Li, 2012; Cheng and Lenkoski, 2012; Lenkoski, 2013; Mohammadi and Wit, 2015) as they allow for full posterior inference.

Inference with the  $G$ -Wishart distribution is challenging. For instance, Wang (2015), Gan et al. (2018), Li et al. (2019) and Sagar K N et al. (2021) obtain major improvements in computational efficiency by replacing the  $G$ -Wishart distribution with shrinkage priors on the precision matrix that enable fast Gibbs sampling updates or EM algorithms. Moreover, building on MCMC methods, SMC (Tan et al., 2017) and unbiased Monte Carlo approximation (van den Boom et al., 2021) have also been considered, as these techniques are *embarrassingly parallel*.

Still working with a  $G$ -Wishart prior, we propose an MCMC algorithm by carefully addressing the major computational bottlenecks in the current literature. Our work builds on advances in MCMC algorithms, in particular, work on delayed Metropolis-Hastings acceptance (Christen and Fox, 2005) and informed proposals (Zanella, 2019) which we extend to the graph literature. First, we propose a delayed acceptance MCMC step to reduce the number of times we need to sample from the  $G$ -Wishart distribution. Such sampling involves iterating a  $O(pd^3)$  algorithm to convergence where  $p$  is the number of nodes and  $d$  the degree of the graph (Lenkoski, 2013). Moreover, we introduce Gibbs updates for the precision matrix enabled by a node reordering which further reduce the need to sample from the  $G$ -Wishart distribution. Finally, we develop an informed proposal distribution for graphs which enables the use of parallel computing environments still in an MCMC framework. As the main distinctive features of the proposed method relate to its

proposal distribution on the graph space, we refer to it as the  $G$ -Wishart weighted proposal algorithm (WWA). We show that WWA improves computation significantly and allows for exploration of larger graph spaces.

The paper is structured as follows. Section 1.1 introduces Bayesian GGMs based on the  $G$ -Wishart prior, while Section 1.2 reviews related literature on posterior inference. Section 2 describes the proposed WWA and contextualises it. Section 3 presents simulation studies to investigate the performance of WWA and compares it with the state of the art. In Section 4, we consider a real data application. We conclude the paper in Section 5.

## 1.1 Model Description

The object of inference is a graph  $G = (V, E)$  defined by a set of edges  $E \subset \{(i, j) \mid 1 \leq i < j \leq p\}$  that represent links among the nodes in  $V = \{1, \dots, p\}$ . In the GGM framework, we have an  $n \times p$  data matrix  $Y$  with independent rows  $Y_i, i = 1, \dots, n$ , corresponding to a  $p$ -dimensional random vector, with its elements represented by nodes on the graph. Each  $Y_i$  is distributed according to a Multivariate Gaussian distribution  $\mathcal{N}(0_{p \times 1}, K^{-1})$  with precision matrix  $K$ . We assume that the precision matrix  $K$  depends on the graph  $G$ : we have that  $K_{ij} = 0$  if nodes  $i$  and  $j$  are not connected, while if there is an edge between two nodes in the graph then the corresponding element of the precision matrix is different from zero with probability one. Thus,  $K \in M^+(G)$  where  $M^+(G)$  is the cone of positive-definite matrices  $K$  with  $K_{ij} = 0$  for  $(i, j) \notin E$ .  $G$  determines the conditional independence structure of the  $p$  variables in  $Y_i, i = 1, \dots, n$ , since  $K_{ij} = 0$  implies that the  $i$ -th and  $j$ -th columns of  $Y$  are independent conditionally on the others by properties of the Multivariate Gaussian distribution.

A popular choice as prior for the precision matrix  $K$  conditional on the graph  $G$  is the  $G$ -Wishart distribution  $\mathcal{W}_G(\delta, D)$  as it induces conjugacy and allows one to work with non-decomposable graphs (Roverato, 2002). It is parametrised by degrees of freedom  $\delta > 2$  and a positive-definite rate matrix  $D$ . Its density is

$$p(K \mid G) = \frac{1}{I_G(\delta, D)} |K|^{\delta/2-1} \exp \left\{ -\frac{1}{2} \text{tr}(K^\top D) \right\}, \quad K \in M^+(G),$$

where  $I_G(\delta, D)$  is a normalising constant. Due to conjugacy,  $K \mid G, Y \sim \mathcal{W}_G(\delta^*, D^*)$ , where

$\delta^* = \delta + n$ ,  $D^* = D + Y^\top Y$ . The model is completed by specifying a prior  $p(G)$  on the graph space. We highlight that the following development does not assume any particular form for  $p(G)$ .

## 1.2 Posterior Distribution

The goal is to compute the posterior distribution (e.g., Atay-Kayis and Massam, 2005)

$$p(G | Y) \propto p(G) \int_{M^+(G)} p(K | G) p(Y | K) dK = \frac{p(G) I_G(\delta^*, D^*)}{(2\pi)^{np/2} I_G(\delta, D)}.$$

The normalising constant  $I_G(\delta, D)$  does not have a simple analytical form for general non-decomposable  $G$ , making evaluation of a Metropolis-Hastings acceptance probability infeasible. To overcome this problem, Monte Carlo (Atay-Kayis and Massam, 2005) and Laplace (Moghaddam et al., 2009; Lenkoski and Dobra, 2011) approximations of  $I_G(\delta, D)$  have been developed. Alternatively, Uhler et al. (2018) provide a recursive expression for  $I_G(\delta, D)$ , but it results in a computationally efficient procedure only for specific types of graphs.

Another line of work avoids direct evaluation of  $I_G(\delta, D)$  through application of the exchange algorithm (Murray et al., 2006) within a broader MCMC. Wang and Li (2012) and Cheng and Lenkoski (2012) employ this strategy in which sampling from the  $G$ -Wishart is performed through a Gibbs step. More recently, Hinne et al. (2014); Mohammadi and Wit (2015); van den Boom et al. (2021) propose methodology based on the exchange algorithm where sampling from  $\mathcal{W}_G(\delta, D)$  is performed through the exact  $G$ -Wishart sampler by Lenkoski (2013), making the algorithm more accurate in terms of exploration of posterior space.

## 2 WWA: $G$ -Wishart Weighted Proposal Algorithm

In this Section, we introduce WWA which advances existing literature by (i) speeding MCMC convergence; (ii) improving the mixing of the chain; (iii) reducing computation time.

---

**Algorithm 1** (Hinne et al., 2014) A single DCBF MCMC Step.

---

**Input:** Graph  $G$ .

**Output:** MCMC update for  $G$  that preserves the posterior  $p(G | Y)$ .

For each edge  $e \in \{(i, j) | 1 \leq i < j \leq p\}$ , do the following:

1. Let  $\tilde{G} = (V, \tilde{E})$  where  $\tilde{E} = E \cup \{e\}$  if  $e \notin E$  and  $\tilde{E} = E \setminus \{e\}$  otherwise.
  2. Reorder the nodes in  $G$  and  $\tilde{G}$  so that  $e$  connects node  $p - 1$  and  $p$ . Rearrange  $D, D^*$  accordingly. Designate all resulting quantities after reordering via a superscript  $e$ .
  3. Draw  $K^e | G, Y \sim \mathcal{W}_{G^e}(\delta^*, D^{*,e})$  and  $\tilde{K}^{0,e} | \tilde{G} \sim \mathcal{W}_{\tilde{G}^e}(\delta, D^e)$ . Compute their respective upper triangular Cholesky decompositions  $\Phi^e$  and  $\tilde{\Phi}^{0,e}$ .
  4. Set  $G = \tilde{G}$  w.p.  $1 \wedge R_{\text{exchange}}$  where  $R_{\text{exchange}}$  is given by Equation (4).
- 

Algorithm 1 describes the double conditional Bayes factor (DCBF) sampler from Hinne et al. (2014). We use DCBF as a prototype for Bayesian algorithms suggested in the literature that allow for posterior inference on non-desomposable graphs, in the context of GGMs with the  $G$ -Wishart prior. In the next three sections, we describe how our strategy allows us to overcome the main bottlenecks of such approaches.

First, we briefly explain the derivation of the acceptance probability of the DCBF sampler. We defer a more extensive and general explanation to Appendix B, where we derive the WWA acceptance probabilities. Let  $K^e = (\Phi^e)^\top \Phi^e$ , where  $\Phi^e$  is an upper triangular matrix and  $K^e$  is obtained from  $K$  by reordering the nodes such that the edge involved in the proposed graph change corresponds to nodes in the last two rows (columns) of  $K^e$ . Let  $\Phi_{ij}^e, i, j \in \{1, \dots, p\}$ , denote the elements of the Cholesky decomposition, and define  $\Phi_{-f}^e := \Phi^e \setminus \{\Phi_{p-1,p}^e, \Phi_{pp}^e\}$ . Then, consider as target the distribution  $p(G, \Phi_{-f}^e | Y)$ , as implied by the full posterior  $p(G, K | Y) \propto p(G) p(K | G) p(Y | K)$ . To compute the acceptance probability in Step 4 of Algorithm 1, we need the the expression (see Cheng and Lenkoski, 2012, for a derivation)

$$\frac{p(Y, \Phi_{-f}^e | \tilde{G})}{p(Y, \Phi_{-f}^e | G)} = N(\Phi_{-f}^e, D^{*,e})^{|\tilde{E}|-|E|} \frac{I_G(\delta, D)}{I_{\tilde{G}}(\delta, D)} \quad (1)$$

where  $N(\Phi_{-f}^e, D^{*,e})$  is an analytically available quantity:

$$N(\Phi_{-f}^e, D^{*,e}) := \Phi_{p-1,p-1}^e \sqrt{\frac{2\pi}{D_{pp}^{*,e}}} \exp \left\{ \frac{D_{pp}^{*,e}}{2} \left( \frac{\Phi_{p-1,p-1}^e D_{p-1,p}^{*,e}}{D_{pp}^{*,e}} - \frac{\sum_{i=1}^{p-2} \Phi_{i,p-1}^e \Phi_{ip}^e}{\Phi_{p-1,p-1}^e} \right)^2 \right\} \quad (2)$$

The ratio in (1) is not of direct use due to the intractable normalising constants  $I_G(\delta, D)$ ,  $I_{\tilde{G}}(\delta, D)$ . The exchange algorithm (Murray et al., 2006) avoids the computation of the normalising constant via the introduction of a Metropolis step defined on an augmented target distribution, which still admits as marginal the desired posterior  $p(G | Y)$ . Specifically, as shown in Step 3 in Algorithm 1, the exchange algorithm requires simulating  $\tilde{K}^{0,e}$  from the  $G$ -Wishart prior based on the proposed graph  $\tilde{G}$ . Let  $\tilde{\Phi}_{-f}^{0,e}$  be defined analogously to  $\Phi_{-f}^e$  and denote its distribution by  $p(\tilde{\Phi}_{-f}^{0,e} | \tilde{G})$ . Consider the distribution defined on the augmented space

$$p(G, \Phi_{-f}^e, \tilde{G}, \tilde{\Phi}_{-f}^{0,e} | Y) \propto p(G, \Phi_{-f}^e | Y) p(\tilde{\Phi}_{-f}^{0,e} | \tilde{G}). \quad (3)$$

DCBF proposes the deterministic exchange  $G \leftrightarrow \tilde{G}$  on the above target. Standard application of detailed balance identifies the acceptance probability as  $1 \wedge R_{\text{exchange}}$ , with

$$\begin{aligned} R_{\text{exchange}} &= \frac{p(\tilde{G}, \Phi_{-f}^e, G, \tilde{\Phi}_{-f}^{0,e} | Y)}{p(G, \Phi_{-f}^e, \tilde{G}, \tilde{\Phi}_{-f}^{0,e} | Y)} = \frac{p(Y, \Phi_{-f}^e | \tilde{G}) p(\tilde{G}) p(\tilde{\Phi}_{-f}^{0,e} | G)}{p(Y, \Phi_{-f}^e | G) p(G) p(\tilde{\Phi}_{-f}^{0,e} | \tilde{G})} \\ &= \frac{p(\tilde{G})}{p(G)} \left\{ \frac{N(\Phi_{-f}^e, D^{*,e})}{N(\tilde{\Phi}_{-f}^{0,e}, D^e)} \right\}^{|\tilde{E}| - |E|} \end{aligned} \quad (4)$$

where the last equality follows from (1).

## 2.1 Full Conditionals for $K$

In Algorithm 1, sampling from the  $G$ -Wishart distributions in Step 3 is computationally expensive. Moreover, sampling from  $\mathcal{W}_{G^e}(\delta^*, D^{*,e})$  can be considerably slower than sampling from  $\mathcal{W}_{\tilde{G}^e}(\delta, D^e)$  under the default hyper-parameter choice  $D = I_p$ . To avoid repeated sampling of the full matrix  $K$ , WWA updates only the elements in the Cholesky decomposition of  $K$  that are affected by the change in the graph. WWA makes use of the following

conditional distributions. First, for  $\Phi_{p-1,p}^e$ ,

$$\Phi_{p-1,p}^e \mid G, \Phi_{-f}^e, Y \sim \mathcal{N} \left( \frac{-\Phi_{p-1,p-1}^e D_{p-1,p}^{*,e}}{D_{p,p}^{*,e}}, \frac{1}{D_{pp}^{*,e}} \right), \quad e \in E, \quad (5a)$$

$$\Phi_{p-1,p}^e \mid G, \Phi_{-f}^e, Y = -\frac{1}{\Phi_{p-1,p-1}^e} \sum_{l=1}^{p-2} \Phi_{l,p-1}^e \Phi_{lp}^e, \quad e \notin E, \quad (5b)$$

where Equation (5a) follows from Equation (5) of van den Boom et al. (2021) and Equation (5b) is Equation (10) of Roverato (2002). For  $\Phi_{pp}^e$ , we derive in Appendix A

$$D_{pp}^{*,e} (\Phi_{pp}^e)^2 \mid G, \Phi_{p-1,p}^e, \Phi_{-f}^e, Y \sim \chi^2(\delta^*). \quad (6)$$

Note that the idea of updating only  $\Phi_{p-1,p}^e$  and  $\Phi_{pp}^e$  has already been mentioned in Cheng and Lenkoski (2012), but as part of an approximate rather than exact MCMC algorithm.

## 2.2 Approximations

We consider the approximation for the ratio of intractable normalising constants derived by Letac et al. (2018) under the default prior choice  $D = I_p$ . That is,

$$\frac{I_G(\delta, D)}{I_{\tilde{G}}(\delta, D)} \approx \left\{ \frac{\Gamma\left(\frac{\delta+d_{\tilde{G}}}{2}\right)}{2\sqrt{\pi}\Gamma\left(\frac{\delta+d_{\tilde{G}}+1}{2}\right)} \right\}^{|\tilde{E}|-|E|} =: \widehat{I_G/I_{\tilde{G}}} \quad (7)$$

where  $d_{\tilde{G}}$  is the number of paths of length two linking the endpoints of edge  $e$ .

Notice that one can avoid working with the extended target in (3), and apply the exchange step  $G \leftrightarrow \tilde{G}$  directly on the target  $p(G, \Phi_{-f}^e \mid Y)$ , with acceptance probability  $1 \wedge R$  where

$$R = \frac{p(\tilde{G}, \Phi_{-f}^e \mid Y)}{p(G, \Phi_{-f}^e \mid Y)} \equiv \frac{p_u(\tilde{G}, \Phi_{-f}^e \mid Y)}{p_u(G, \Phi_{-f}^e \mid Y)} \times \frac{I_G(\delta, D)}{I_{\tilde{G}}(\delta, D)} \quad (8)$$

for the analytically available unnormalised densities  $p_u(\cdot, \cdot \mid \cdot)$  defined in the obvious way via (1). From (7), (8), one can obtain the approximation

$$\widehat{R} \equiv \widehat{R}(G, \tilde{G}, K) := \frac{p_u(\tilde{G}, \Phi_{-f}^e \mid Y)}{p_u(G, \Phi_{-f}^e \mid Y)} \times \widehat{I_G/I_{\tilde{G}}} \quad (9)$$



We make use of this approximation both within the development of our informed proposal and for the introduction of a delayed acceptance step within WWA. Combining (1), (8) leads to an explicit expression for  $\widehat{R}$ :

$$\widehat{R} = \frac{p(\widetilde{G})}{p(G)} \left\{ N(\Phi_{-f}^e, D^{*,e}) \frac{\Gamma\left(\frac{\delta+d_{\widetilde{G}}}{2}\right)}{2\sqrt{\pi} \Gamma\left(\frac{\delta+d_{\widetilde{G}}+1}{2}\right)} \right\}^{|\widetilde{E}|-|E|}$$

### 2.3 Informed Proposal

WWA improves MCMC convergence and mixing per  $G$ -Wishart sample through the use of a proposal distribution that is informed by the target. We will first describe a simple modification at the proposal that is blind to the target, before proceeding to the description of the informed approach.

First, notice that at every MCMC iteration, Algorithm 1 scans through all the edges. At each such substep, it proposes graph  $\widetilde{G}$  with the edge removed if it is present in the current graph  $G$ , or vice versa. This is similar in rational to specifying a uniform proposal distribution  $q(\widetilde{G} | G)$  on which edge to flip. That is,  $q(\widetilde{G} | G) = 1/m_{\max}$  for  $\widetilde{G} \in \text{nbnd}(G)$  where  $m_{\max} = p(p-1)/2$  denotes the maximum number of edges and the neighbourhood  $\text{nbnd}(G)$  is the set of  $m_{\max}$  graphs that differ from  $G$  by exactly one edge. A downside of the uniform proposal is that the probability of removing an edge equals  $|E|/m_{\max}$  which is usually small, especially when a shrinkage prior on graphs is used. A possible solution is offered by Dobra et al. (2011) who first propose to remove or add an edge with probability 0.5 and then pick an edge uniformly at random from the appropriate subset. Obviously, for  $|E| \in \{0, m_{\max}\}$ , we propose to add and remove an edge, accordingly. This results in the proposal

$$q(\widetilde{G} | G) = \begin{cases} \frac{1}{m_{\max}}, & |E| = 0, m_{\max}, \\ \frac{1}{2|E|}, & |\widetilde{E}| < |E| \neq m_{\max}, \\ \frac{1}{2(m_{\max}-|E|)}, & |\widetilde{E}| > |E| \neq 0, \end{cases} \quad (10)$$

for  $\widetilde{G} \in \text{nbnd}(G)$ .

Second, and most importantly, WWA makes use of a proposal for the graph that learns from the target. Locally balanced proposals (Zanella, 2019) provide inspiration to further

improve  $q(\tilde{G} | G)$  defined above. Such proposals are informed by an *embarrassingly parallel* scan through the neighbourhood of the current discrete state in a Markov chain. Specifically, denote the current and proposed states by  $x$  and  $\tilde{x}$ , respectively, the target distribution by  $\pi(x)$  and some baseline proposal by  $q(\tilde{x} | x)$ . Then, an informed proposal  $Q(\tilde{x} | x)$  is defined by

$$Q(\tilde{x} | x) \propto g \left\{ \frac{\pi(\tilde{x})}{\pi(x)} \right\} q(\tilde{x} | x), \quad (11)$$

for some balancing function  $g(t)$ . Here, the transition kernel  $Q(\tilde{x} | x)$  is locally balanced if and only if  $g(t) = t g(1/t)$  (Zanella, 2019). The role of the balancing function is to redirect the proposal towards candidates of high posterior probability. The aggressiveness of the redirection is determined by the shape of  $g(\cdot)$ . In practice, best MCMC mixing results from a balance between information from the neighbourhood scan, which concentrates the proposal, and the diffuseness of the proposal. The use of an informed proposal in a Metropolis-Hastings acceptance probability requires the normalising constant of  $Q(\tilde{x} | x)$ . Computing the constant involves computing  $\pi(\tilde{x})/\pi(x)$  for all  $\tilde{x}$  in the support of  $q(\tilde{x} | x)$ . This task is *embarrassingly parallel*.

WWA develops an informed proposal in the context of GGMs with  $q(\tilde{G} | G)$  in Equation (10) as baseline proposal. We note that the ratio  $\pi(\tilde{x})/\pi(x)$  in (11) only serves to improve the proposal. Instead, we use the analytically available approximation of the ratio of targets  $\hat{R}$  in (9). Notice that this ratio involves the current precision matrix  $K$ . That is, we have

$$\begin{aligned} Q(\tilde{G} | G, K) &:= C(G, K) \cdot g \left\{ \frac{p_u(\tilde{G}, \Phi_{-f}^e | Y)}{p_u(G, \Phi_{-f}^e | Y)} \times \widehat{I_G / I_{\tilde{G}}} \right\} q(\tilde{G} | G) \\ &= C(G, K) \cdot g \left\{ \hat{R}(G, \tilde{G}, K) \right\} q(\tilde{G} | G), \end{aligned} \quad (12)$$

for a normalising constant  $C(G, K)$ . Thus, the informed proposal for  $\tilde{G}$  has the form  $Q(\tilde{G} | G, K)$ , differently from Zanella (2019) where the informed proposal only depends on the discrete state. Moreover, in the GGM context an update on the graph leads to an update on the precision matrix (with a distribution defined on a continuous space). Such considerations are carefully addressed in Appendix B to ensure correctness of the deduced MCMC.

## 2.4 Delayed Acceptance

We will make use of the approximation  $\widehat{R}$  in (9) for the introduction of a delayed acceptance (DA) step (Christen and Fox, 2005) within WWA. We develop the DA approach, by applying the idea of targeting  $p(G, \Phi_{-f}^e | Y)$ , with a proposed exchange  $G \leftrightarrow \widetilde{G}$  based on the kernel  $Q(\widetilde{G} | G, K)$  in (12), and a simultaneous exchange between  $K \leftrightarrow \widetilde{K}$  where  $\widetilde{K}$  involves the constituent elements  $\widetilde{\Phi}_{-f}^e = \Phi_{-f}^e$ ,  $\widetilde{\Phi}_{pp}^e = \Phi_{pp}^e$  (i.e., the same as the corresponding elements of  $K$ ) and sampling  $\widetilde{\Phi}_{p-1,p}^e$  according to (5).

Following the DA idea, the approximation  $\widehat{R}$  in (9) will be used in place of the ratio of targets. That is, we ‘promote’ a proposed  $\widetilde{G}$  with acceptance probability  $1 \wedge \widehat{R}_{\text{DA}}$ , where

$$\begin{aligned} \widehat{R}_{\text{DA}} &:= \frac{p_u(\widetilde{G}, \Phi_{-f}^e | Y)}{p_u(G, \Phi_{-f}^e | Y)} \times \widehat{I_G / I_{\widetilde{G}}} \times \frac{Q(G | \widetilde{G}, \widetilde{K})}{Q(\widetilde{G} | G, K)} \\ &= \widehat{R} \times \frac{Q(G | \widetilde{G}, \widetilde{K})}{Q(\widetilde{G} | G, K)} \end{aligned} \tag{13}$$

This promotion step provides a speed-up over the exchange algorithm of acceptance probability  $1 \wedge R_{\text{exchange}}$  by not having to sample from  $\mathcal{W}_{\widetilde{G}}(\delta, D)$ , at the cost of targeting the wrong distribution. Use of the complete machinery of the DA MCMC in the WWA algorithm corrects for this inconsistency (see Algorithm 2).

DA has been originally developed to employ approximate posteriors within an exact MCMC, while we directly approximate the acceptance ratio. Specifically, our use of DA involves first a Metropolis-Hastings step with approximate acceptance ratio. Then, the outcome is treated as proposal in a second (delayed) accept-reject step that uses the exact ratio in (4). This has the advantage that one only needs to perform the exchange algorithm when an acceptance in the approximate Metropolis-Hastings is achieved. This implies that ‘poor’ proposed graphs get rejected quickly and more computational effort is spent on regions of the space with high posterior probability.

## 2.5 The Complete WWA Algorithm

Algorithm 2 details the WWA algorithm. A proposed  $\widetilde{G}$  is associated with a  $\widetilde{K}$  as the graph imposes a sparsity pattern on the precision matrix. To ensure detailed balance,  $\widetilde{K}$  appears

---

**Algorithm 2** A Single WWA MCMC Step.

---

**Input:** Graph  $G$ .

**Output:** MCMC update for  $G$  such that the invariant distribution is the posterior  $p(G | Y)$ .

1. Draw  $K | G, Y \sim \mathcal{W}_G(\delta^*, D^*)$ .
2. Repeat the following single-edge update a number of times  $n_E$ :
  - (a) Sample  $\tilde{G}$  from the informed proposal  $Q(\tilde{G} | G, K)$  given by (12) with  $g(t) = t/(1+t)$ .
  - (b) Denote the edge in which  $G$  and  $\tilde{G}$  differ by  $e$ . Reorder the nodes in  $G$  and  $\tilde{G}$  so that  $e$  connects node  $p-1$  and  $p$ . Rearrange  $K$ ,  $D$  and  $D^*$  accordingly. Denote the resulting quantities with a superscript  $e$ .
  - (c) Denote the upper triangular Cholesky decomposition of  $K^e$  by  $\Phi^e$ . Update  $\Phi_{pp}^e$  according to (6).
  - (d) Generate a  $\tilde{K}^e$  corresponding with  $\tilde{G}^e$  from  $K$ , by setting  $\tilde{\Phi}_{-f}^e = \Phi_{-f}^e$ ,  $\tilde{\Phi}_{pp}^e = \Phi_{pp}^e$ , and sampling  $\tilde{\Phi}_{p-1,p}^e$  according to (5).
  - (e) Compute  $Q(G | \tilde{G}, \tilde{K})$ .
  - (f) ‘Promote’  $\tilde{G}$  to be considered for delayed acceptance w.p.  $1 \wedge \hat{R}_{\text{DA}}$ , where  $\hat{R}_{\text{DA}}$  is given by (13). If  $\tilde{G}$  is promoted:
    - i. Sample  $\tilde{K}^{0,e} | \tilde{G} \sim \mathcal{W}_{\tilde{G}^e}(\delta, D^e)$ .
    - ii. Set  $G = \tilde{G}$  and  $K = \tilde{K}$  w.p.  $1 \wedge R_{\text{DA}}$  where

$$R_{\text{DA}} = R_{\text{exchange}} \frac{(1 \wedge \hat{R}_{\text{DA}}^{-1}) Q(G | \tilde{G}, \tilde{K})}{(1 \wedge \hat{R}_{\text{DA}}) Q(\tilde{G} | G, K)}$$

where  $R_{\text{exchange}}$  is given by (4).

---

in the computation of the reverse probability  $Q(G | \tilde{G}, \tilde{K})$ . As such, the MCMC update needs to be joint on  $K$  and  $G$  where the dimensionality  $p + |E|$  of the continuous state space of  $K$  varies with  $G$ , since every time we remove or add an edge the number of free parameters in  $K$  changes. In Appendix B, the resulting acceptance probability is derived via reversible jump MCMC (Green, 1995) to account for the transdimensionality.

In Sections 3 and 4, we employ the balancing function  $g(t) = t/(1 + t)$  as suggested by Zanella (2019), although the algorithm is well defined for any  $g$ . In our experiments, we also consider  $g(t) = \sqrt{t}$  as its unboundedness might help convergence. We find that this alternative choice results in both worse convergence and mixing (results not shown).

In Appendix B, we derive the acceptance probabilities involved in Step 2f. The relative computational cost of sampling from  $\mathcal{W}_G(\delta^*, D^*)$  in Step 1 becomes negligible if the number of single edge updates  $n_E$  is sufficiently large, e.g.  $n_E = p$ . Then, the embarrassingly parallel computation of the informed proposal in Steps 2a and 2e, and the sampling from  $\mathcal{W}_{\tilde{G}}(\delta, D)$  in Step 2(f)i carry the vast majority of computational cost (in most applications more than 90%).

To efficiently sample from the  $G$ -Wishart distribution in WWA, we combine graph decomposition with the  $G$ -Wishart sampler of Lenkoski (2013). The main idea is as follows: first, we split the graph into connected components as sampling of the rows and columns of the precision matrix can be done independently for each connected component. Note that each independent component can be sampled from a  $G$ -Wishart of appropriate dimension, as the entire precision matrix can be rewritten as a block matrix.  $G$ -Wishart sampling for a connected component proceeds using a perfectly ordered clique minimal separator decomposition (see, for example, Berry et al., 2010, for an introduction to graph decomposition) as detailed in Wang and Carvalho (2010). Note that Carvalho et al. (2007) first mention the idea of sampling from the  $G$ -Wishart exploiting a decomposition of the graph. We opt for the MCSM-Atom-Tree algorithm of Berry et al. (2014) to compute a perfectly ordered clique minimal separator decomposition at negligible cost. The decomposition splits the graphs in complete (i.e. cliques) and incomplete prime graphs. In the first case, we can use a standard Wishart sampler, while the latter requires sampling

from a  $G$ -Wishart. WWA uses the  $G$ -Wishart sampler of Lenkoski (2013) for the incomplete prime graphs. The rejection sampler of Wang and Carvalho (2010) is an alternative for small incomplete prime graphs where it can be faster, but any speed-up would be negligible as the main computational cost derives from sampling large incomplete prime graphs.

WWA requires a reordering of the nodes in Step 2b as explained in Section 2.1. In Step 2c, we update  $\Phi_{pp}^e$ , which is not necessary for a valid MCMC as its distribution does not depend on the edge  $e$  being in the graph or not. Nonetheless, WWA includes it as its computational cost is negligible and it improves mixing, especially for a large number of single edge updates  $n_E$ . The CL algorithm in Cheng and Lenkoski (2012) also includes the step.

## 2.6 Related Work

In this Section, we contextualise WWA in reference to previous work on MCMC for graphs. Wang and Li (2012) and Cheng and Lenkoski (2012) also consider doing a single edge update many times for each full update of  $K$ , as in Step 2 of Algorithm 2. Additionally, they describe a two stage procedure that resembles delayed acceptance. In Appendix C, we describe the CL algorithm of Cheng and Lenkoski (2012). Its first accept-reject step (for individual edges) uses Barker’s algorithm (Barker, 1965) with acceptance ratio  $R_{\text{exchange}}$  given in (4) where the term  $N(\tilde{\Phi}_{-f}^{0,e}, D^e)$  is set to one. To correct for this approximation, they, then, introduce a second Metropolis-Hastings accept-reject step. This combination of steps is, in fact, a delayed acceptance, but both Wang and Li (2012) and Cheng and Lenkoski (2012) do not explicitly justify it as such. Effectively, they approximate the ratio of normalising constants by one while WWA uses (7).

WWA’s computation of the informed proposal  $Q(\tilde{G} \mid G, K)$  is embarrassingly parallel. In this respect, so is the calculation of birth and death rates in Mohammadi and Wit (2015). Moreover, The R package `BDgraph` (Mohammadi and Wit, 2019) approximates these rates using (7) by default, which is the same approximation used for  $Q(\tilde{G} \mid G, K)$  in Step 2a of Algorithm 2. Unlike WWA, `BDgraph` does not correct for the fact that it uses an approximation.

The embarrassingly parallel search through the neighbourhood  $\text{nbd}(G)$ , which constitutes  $Q(\tilde{G} \mid G, K)$ , is reminiscent of the parallel computation enabled by shotgun stochastic search (SSS, Hans et al., 2007). Jones et al. (2005) apply SSS for stochastic search on graph space using an approximate likelihood for GGMs. WWA similarly enables parallel computing in an MCMC framework, while still using the exact likelihood.

### 3 Simulation Studies

We compare WWA (Algorithm 2) with DCBF (Algorithm 1) as DCBF can be considered the state of the art for MCMC in GGMs with a  $G$ -Wishart distribution as shown by Hinne et al. (2014). We choose  $n_E = p$  for the number of single edge updates in Algorithm 2. To bring the computational cost of Algorithm 1 more in line with WWA and for a fairer comparison, we slightly modify DCBF: instead of executing the steps in Algorithm 1 for all  $m_{\max}$  possible edges, we execute them for  $p$  edges drawn uniformly at random with replacement.

To measure MCMC efficiency, we use as metric the cost of an independent sample, that is the computation time required for a unit increase in the effective sample size (Fang et al., 2020):

$$\begin{aligned} \text{cost of an independent sample} &= \frac{\text{number of MCMC steps}}{\text{effective sample size}} \times \text{cost per step} \\ &= \text{integrated autocorrelation time} \times \text{cost per step} \end{aligned}$$

This captures MCMC mixing and adjusts for computational cost. MCMC convergence can additionally be a computational bottleneck especially if an effective initialisation is not available. Therefore, we also discuss convergence issues in Section 4. The integrated autocorrelation time is computed for the number of edges  $|E|$  using the R package `LaplacesDemon` (Statisticat, LLC., 2020). The cost of the embarrassingly parallel computation of the informed proposal in Steps 2a and 2e of Algorithm 2 is assessed based on 128 CPU cores. To make computation times comparable, all methods are implemented in C++ and use the same routines as much as possible, for instance, to sample from the  $G$ -Wishart distribution.

### 3.1 Cycle Graphs

A major improvement in computational cost from WWA over DCBF derives from reducing the number of times we need to sample from the  $G$ -Wishart distribution. The gains associated with WWA will thus be larger if  $G$ -Wishart sampling is slower. This situation arises, for example, when  $G$  contains large incomplete prime graphs. To highlight this point, we consider cycle graphs, which are themselves incomplete prime graphs. We follow Section 6.2 of Wang and Li (2012) to simulate data from cycle graphs. In the  $G$ -Wishart prior, we set  $\delta = 3$  and  $D = I_p$ . The edges are a priori independent with edge inclusion probability  $\rho = 2/(p-1)$ . That is,  $p(G) = \rho^{|E|}(1-\rho)^{m_{\max}-|E|}$ . We simulate  $n = \frac{3}{2}p$  random vectors  $Y_i$  from  $\mathcal{N}(0_{p \times 1}, K^{-1})$  with a precision matrix  $K$  given by  $K_{ii} = 1$  for  $i = 1, \dots, p$ ,  $K_{ij} = 0.5$  for  $|i-j| = 1$ ,  $K_{1p} = K_{p1} = 0.4$  and all other elements being equal to zero. We simulate data for  $p = 10, 20, 40$ . The performance of the two algorithms is assessed over 32 replicates of the simulations.

We run the MCMC for 11,000 iterations, discarding the first 1,000 as burn-in. We initialise the graph at the true cycle for all algorithms. We compare the performance of WWA with (i) DCBF; (ii) WWA without the delayed acceptance and the informed proposal; (iii) WWA with delayed acceptance, but without the informed proposal; and (iv) WWA with the informed proposal, but without delayed acceptance. When we do not use the informed proposal, we set  $q(\tilde{G} | G)$  equal to (10). When we do not perform delayed acceptance in WWA, we use the acceptance probability in Step 4 of Algorithm 1 directly. These extra comparisons provide insight into the role of the different innovations of the WWA.

Figure 1 shows that WWA provides more efficient posterior computation than DCBF on these simulated data. This difference increases with the number of nodes with WWA being 12 times more efficient than DCBF for  $p = 40$  nodes. The MCMC without the informed proposal outperforms WWA for  $p = 40$ . This is probably a result of the informed proposal and the delayed acceptance both relying on the same approximation in (7): the informed proposal, compared to the base proposal  $q(\tilde{G} | G)$ , increases the acceptance ratio of the first approximate accept-reject step in DA MCMC, but this increased acceptance does not translate to a proportional increase in the overall acceptance ratio. These effects are compounded



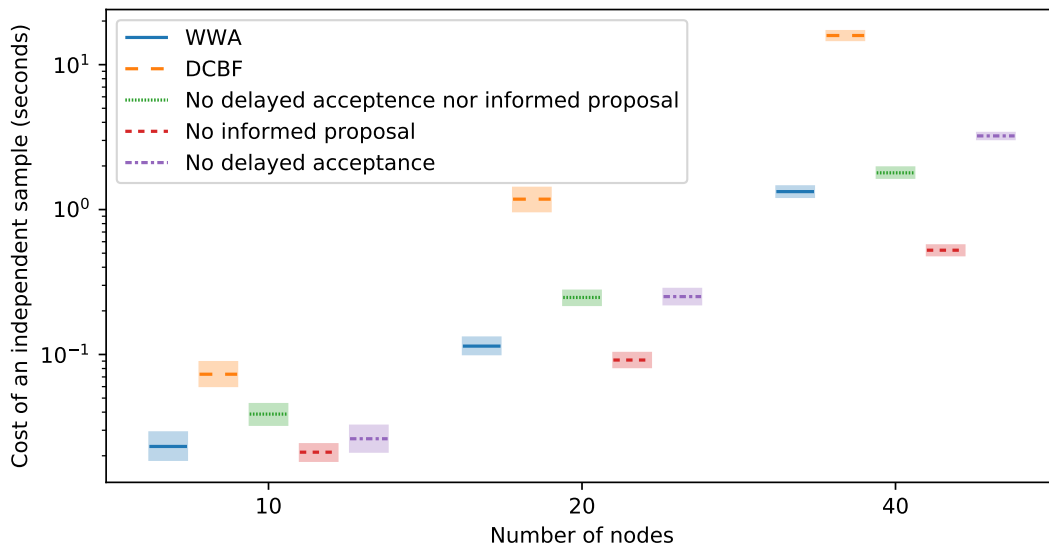


Figure 1: Cost of posterior computations versus the number of nodes for the data simulated from a cycle graph. The lines represent means over the 32 repetitions for DCBF and WWA as well as different specifications of WWA. The shaded areas are 95% bootstrapped confidence intervals.

by the approximation in (7) becoming less accurate for larger graphs (Letac and Massam, 2007). The result is that Step 2(f)i of Algorithm 2, which involves the relatively expensive sampling from  $\mathcal{W}_{\tilde{G}}(\delta, D)$ , is evaluated more often without a corresponding improvement in MCMC mixing, i.e. the gain in mixing from the informed proposal does not compensate for this extra sampling.

### 3.2 Uniformly Sampled Graphs

In this Section, we compare the performance of the different algorithms on data simulated from the Bayesian model described in Section 1.1 with  $n = 2p$  and a uniform prior on graphs:  $p(G) = 2^{-m_{\max}}$ . In particular, we generate the graphs from this uniform distribution. We show results for 32 replicates and for  $p = 10, 20, 40$ . MCMC is initialised at the true graph  $G$ . The remaining set-up of this simulation study follows Section 3.1.

Also in this simulation scenario, WWA provides more efficient posterior computation

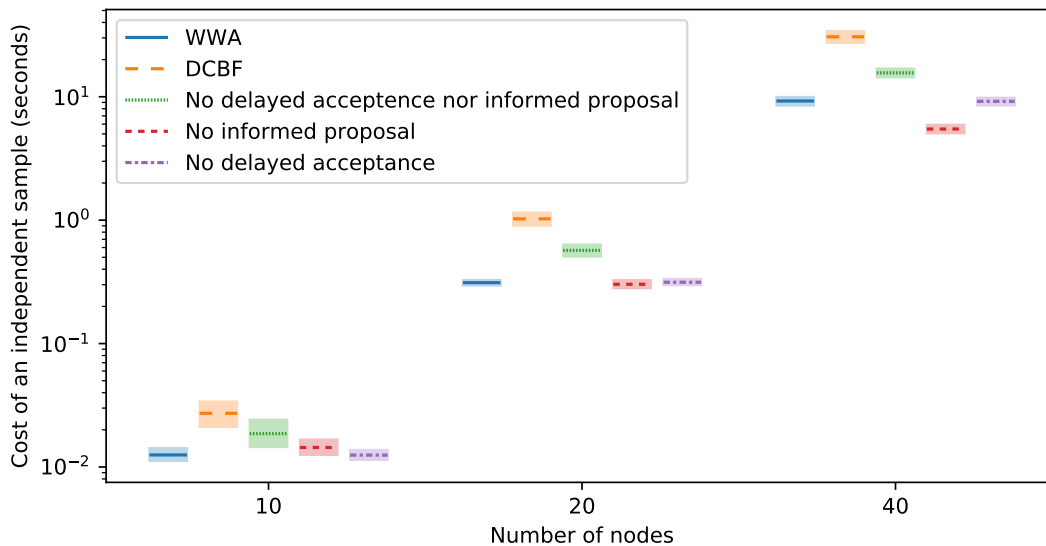


Figure 2: Cost of posterior computations versus the number of nodes for the data simulated from a uniformly sampled graph. The lines represent means over the 32 repetitions for DCBF and WWA as well as different specifications of WWA. The shaded areas are 95% bootstrapped confidence intervals.

than DCBF as shown in Figure 2. Again, this difference increases with the number of nodes with WWA being 3.3 times more efficient than DCBF for  $p = 40$  nodes. As in Section 3.1, the MCMC without the informed proposal outperforms WWA for  $p = 40$ .

## 4 Application to Gene Expression Data

We consider the real data application from Section 4.2 of Mohammadi and Wit (2015) where a more extensive data description is available. The data consist of gene expressions in B-lymphocyte cells (Stranger et al., 2007) from  $n = 60$  individuals. They are quantile-normalised to marginally follow a standard Gaussian distribution, a process also known as rank normalisation. We consider two data sets  $Y$ , namely those consisting of the  $p = 50$  and  $p = 100$  most variable gene expressions. The prior on  $(G, K)$  is the same as in Section 3.2, which coincides with an uninformative prior.

For  $p = 50$ , WWA and DCBF are initialised at a graphical lasso estimate of the graph  $G$

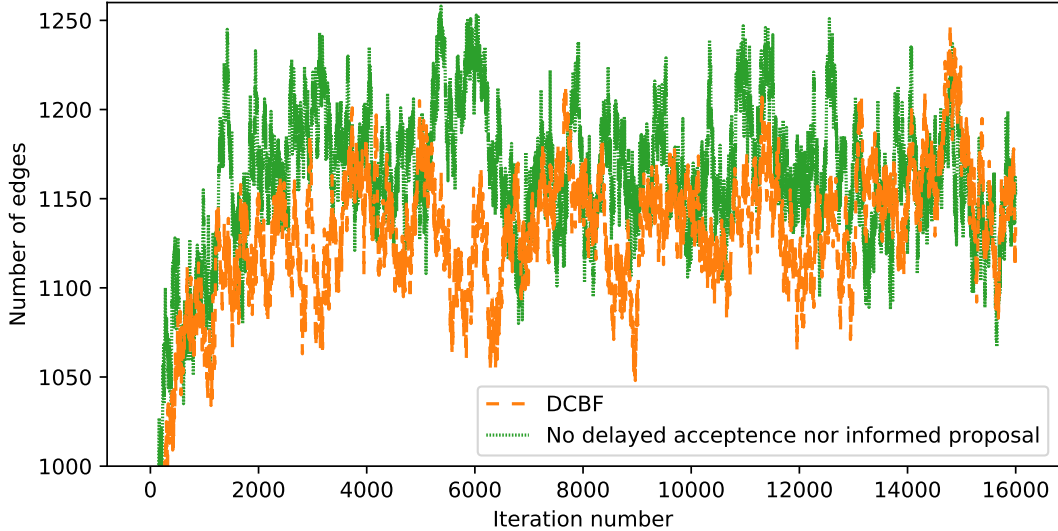


Figure 3: Trace plots for the number of edges in the gene expression application with  $p = 100$  nodes.

(Friedman et al., 2007) and are run for 16,000 iterations of which the last 10,000 are used to estimate the cost of an independent sample. For the data set with  $p = 100$ , the number of possible graphs is  $2^{m_{\max}} = 1.3 \cdot 10^{1,490}$ , and the precision matrix is not identifiable in the likelihood since  $n < p$ . Although this is not theoretically a problem in the Bayesian framework, because of prior regularisation, likelihood unidentifiability is known to cause problems for MCMC convergence. Also, the approximation in (7) favours sparse graphs as it is consistently biased in this direction (Letac et al., 2018, page 5), a tendency which is rather strong when the posterior is not concentrated as in the case of  $p = 100$ . As a result, using the informed proposal or delayed acceptance based on (7) results in bad MCMC convergence and mixing. Therefore, we use Algorithm 2 without the informed proposal nor delayed acceptance because the bias in the approximation would dominate the information deriving from the posterior which is flat in this example.

In terms of speed, the first 6,000 burn-in iterations take 11 minutes for WWA versus 36 minutes for DCBF with  $p = 50$ , and 4.1 hours for the proposed algorithm versus 9.0 hours for DCBF with  $p = 100$ . We compute the improved  $\hat{R}$  of Vehtari et al. (2021) as a

diagnostic of convergence on the last 10,000 iterations.  $\widehat{R}$  converges to one as the number of iterations tends to infinity and  $\widehat{R} > 1.01$  indicates lack of convergence. For  $p = 50$ , when the precision matrix is likelihood identifiable as well, convergence is reached quickly by both algorithms with  $\widehat{R} = 1.003$  for WWA and  $\widehat{R} = 1.006$  for DCBF. For  $p = 100$ , the trace plots in Figure 3 show an increasing trend for the number of edges for DCBF, indicating slower convergence confirmed by  $\widehat{R} = 1.068$ . This contrasts with the proposed algorithm where  $\widehat{R} = 1.001$  and which seems to converge within 2,000 iterations. The introduced methodology yields faster MCMC convergence, both in terms of number of iterations and especially in terms of computation time.

WWA is also superior to DCBF in terms of MCMC mixing. For  $p = 100$ , we run DCBF for 10,000 iterations initialised at the last iteration of the proposed algorithm, to avoid DCBF’s convergence issues while assessing MCMC mixing. The cost of an independent sample is 6.2 seconds for WWA versus 24 seconds for DCBF with  $p = 50$ , and 7.4 minutes for the proposed algorithm versus 14 minutes for DCBF with  $p = 100$ .

## 5 Discussion

In this work, we propose WWA, a novel algorithm for GGMs which significantly improves over existing MCMC based on the  $G$ -Wishart prior. The main contributions involve delayed acceptance, Gibbs updates for the precision matrix, and the use of parallel computing to inform the proposal. As a result, WWA outperforms the state-of-the-art alternative in terms of MCMC mixing, convergence and computation time.

Here, we discuss possible improvements and extensions to WWA. As the number of nodes increases, normalising the informed proposal takes longer, with the added computational cost potentially outweighing the improvement in MCMC mixing. A potential extension to tune this computation versus mixing trade-off is blocking (Zanella, 2019). It constrains the support of the informed proposal to a subset or ‘block’ of the neighbourhood of a graph, reducing computational cost of normalising the informed proposal.

Another improvement to the informed proposal would be a faster or more accurate approximation than (9). The computational bottleneck of the current approximation is cal-

culating the Cholesky decomposition  $\Phi^e$ . For sparse graphs, the Cholesky decomposition can be sped up via fill-in reducing node reorderings, which increase sparsity in  $\Phi^e$ , and Cholesky routines optimised for sparse matrices (Rue, 2001; Rue and Held, 2005, Section 2.4.3) as shown by Cheng and Lenkoski (2012).

The MCMC performance is limited by the fact that at most one edge is changed for each accept-reject step. A truly scalable algorithm requires larger moves in the graph space as the number of possible edges in a graph is quadratic in the number of nodes. Such larger moves require sufficiently good proposals, for both the graph and the precision matrix  $K$ . Tan et al. (2017) take a first step in this direction by changing multiple edges at the same time with an approximate likelihood on the graph resulting from approximating  $I_G(\delta, D)$ .

In this work, we focus on GGMs because of their popularity in applications and the computational challenges associated with their estimation. Due to the modular nature of MCMC, WWA can also provide a feasible strategy in extended models such as multiple graphs (e.g., Peterson et al., 2015; Tan et al., 2017), Gaussian copulas to accommodate non-Gaussian data (e.g., Dobra and Lenkoski, 2011; Mohammadi and Wit, 2019) or sparse seemingly unrelated regressions (e.g., Wang, 2010; Bhadra and Mallick, 2013).

## SUPPLEMENTARY MATERIAL

**Code:** The scripts that produced the empirical results are available at <https://github.com/willemvandenboom/wwa>. (GitHub repository)

## References

- Atay-Kayis, A. and H. Massam (2005). A Monte Carlo method for computing the marginal likelihood in nondecomposable Gaussian graphical models. *Biometrika* 92(2), 317–335.
- Barker, A. A. (1965). Monte Carlo calculations of the radial distribution functions for a proton-electron plasma. *Australian Journal of Physics* 18(2), 119.
- Berry, A., R. Pogorelnik, and G. Simonet (2010). An introduction to clique minimal separator decomposition. *Algorithms* 3(2), 197–215.

- Berry, A., R. POGORELNIK, and G. SIMONET (2014). Organizing the atoms of the clique separator decomposition into an atom tree. *Discrete Applied Mathematics* 177, 1–13.
- Bhadra, A. and B. K. MALICK (2013). Joint high-dimensional Bayesian variable and covariance selection with an application to eQTL analysis. *Biometrics* 69(2), 447–457.
- Bornn, L. and F. CARON (2011). Bayesian clustering in decomposable graphs. *Bayesian Analysis* 6(4), 829–846.
- Carvalho, C. M., H. MASSAM, and M. WEST (2007). Simulation of hyper-inverse Wishart distributions in graphical models. *Biometrika* 94(3), 647–659.
- Cheng, Y. and A. LENKOSKI (2012). Hierarchical Gaussian graphical models: Beyond reversible jump. *Electronic Journal of Statistics* 6, 2309–2331.
- Christen, J. A. and C. FOX (2005). Markov chain Monte Carlo using an approximation. *Journal of Computational and Graphical Statistics* 14(4), 795–810.
- Dawid, A. P. and S. L. LAURITZEN (1993). Hyper Markov laws in the statistical analysis of decomposable graphical models. *The Annals of Statistics* 21(3), 1272–1317.
- Dempster, A. P. (1972, March). Covariance selection. *Biometrics* 28(1), 157.
- Dobra, A. and A. LENKOSKI (2011). Copula Gaussian graphical models and their application to modeling functional disability data. *The Annals of Applied Statistics* 5(2A), 969–993.
- Dobra, A., A. LENKOSKI, and A. RODRIGUEZ (2011). Bayesian inference for general Gaussian graphical models with application to multivariate lattice data. *Journal of the American Statistical Association* 106(496), 1418–1433.
- Fang, Y., Y. CAO, and R. D. SKEEL (2020). Quasi-reliable estimates of effective sample size. *IMA Journal of Numerical Analysis* (draa077).
- Fitch, A. M., M. B. JONES, and H. MASSAM (2014). The performance of covariance selection methods that consider decomposable models only. *Bayesian Analysis* 9(3), 659–684.

- Friedman, J., T. Hastie, and R. Tibshirani (2007). Sparse inverse covariance estimation with the graphical lasso. *Biostatistics* 9(3), 432–441.
- Gan, L., N. N. Narisetty, and F. Liang (2018). Bayesian regularization for graphical models with unequal shrinkage. *Journal of the American Statistical Association* 114(527), 1218–1231.
- Giudici, P. and P. J. Green (1999). Decomposable graphical Gaussian model determination. *Biometrika* 86(4), 785–801.
- Green, P. J. (1995). Reversible jump Markov chain Monte Carlo computation and Bayesian model determination. *Biometrika* 82(4), 711–732.
- Hans, C., A. Dobra, and M. West (2007). Shotgun stochastic search for “large  $p$ ” regression. *Journal of the American Statistical Association* 102(478), 507–516.
- Hinne, M., A. Lenkoski, T. Heskes, and M. van Gerven (2014). Efficient sampling of Gaussian graphical models using conditional Bayes factors. *Stat* 3(1), 326–336.
- Jones, B., C. Carvalho, A. Dobra, C. Hans, C. Carter, and M. West (2005). Experiments in stochastic computation for high-dimensional graphical models. *Statistical Science* 20(4), 388–400.
- Khare, K., B. Rajaratnam, and A. Saha (2018). Bayesian inference for Gaussian graphical models beyond decomposable graphs. *Journal of the Royal Statistical Society: Series B (Statistical Methodology)* 80(4), 727–747.
- Lauritzen, S. L. (1996). *Graphical Models*. Oxford Statistical Science Series. The Clarendon Press, Oxford University Press, New York.
- Lenkoski, A. (2013). A direct sampler for G-Wishart variates. *Stat* 2(1), 119–128.
- Lenkoski, A. and A. Dobra (2011). Computational aspects related to inference in Gaussian graphical models with the G-Wishart prior. *Journal of Computational and Graphical Statistics* 20(1), 140–157.

- Letac, G. and H. Massam (2007). Wishart distributions for decomposable graphs. *The Annals of Statistics* 35(3), 1278–1323.
- Letac, G., H. Massam, and R. Mohammadi (2018). The ratio of normalizing constants for Bayesian graphical Gaussian model selection. arXiv:1706.04416v2.
- Li, Y., B. A. Craig, and A. Bhadra (2019). The graphical horseshoe estimator for inverse covariance matrices. *Journal of Computational and Graphical Statistics* 28(3), 747–757.
- Moghaddam, B., E. Khan, K. P. Murphy, and B. M. Marlin (2009). Accelerating Bayesian structural inference for non-decomposable Gaussian graphical models. In Y. Bengio, D. Schuurmans, J. Lafferty, C. Williams, and A. Culotta (Eds.), *Advances in Neural Information Processing Systems*, Volume 22. Curran Associates, Inc.
- Mohammadi, A. and E. C. Wit (2015). Bayesian structure learning in sparse Gaussian graphical models. *Bayesian Analysis* 10(1), 109–138.
- Mohammadi, R. and E. C. Wit (2019). BDgraph: An R package for Bayesian structure learning in graphical models. *Journal of Statistical Software* 89(3).
- Murray, I., Z. Ghahramani, and D. J. C. MacKay (2006). MCMC for doubly-intractable distributions. In *Proceedings of the Twenty-Second Conference on Uncertainty in Artificial Intelligence*, UAI’06, Arlington, Virginia, USA, pp. 359–366. AUAI Press.
- Niu, Y., D. Pati, and B. K. Mallick (2021). Bayesian graph selection consistency under model misspecification. *Bernoulli* 27(1), 636–672.
- Peterson, C., F. C. Stingo, and M. Vannucci (2015). Bayesian inference of multiple Gaussian graphical models. *Journal of the American Statistical Association* 110(509), 159–174.
- Roverato, A. (2002). Hyper inverse Wishart distribution for non-decomposable graphs and its application to Bayesian inference for Gaussian graphical models. *Scandinavian Journal of Statistics* 29(3), 391–411.
- Rue, H. (2001). Fast sampling of Gaussian Markov random fields. *Journal of the Royal Statistical Society: Series B (Statistical Methodology)* 63(2), 325–338.



- Rue, H. and L. Held (2005). *Gaussian Markov Random Fields*. New York: Chapman and Hall/CRC.
- Sagar K N, K., S. Banerjee, J. Datta, and A. Bhadra (2021). Precision matrix estimation under the horseshoe-like prior-penalty dual. arXiv:2104.10750v1.
- Scott, J. G. and C. M. Carvalho (2008). Feature-inclusion stochastic search for Gaussian graphical models. *Journal of Computational and Graphical Statistics* 17(4), 790–808.
- Statisticat, LLC. (2020). *LaplacesDemon: Complete Environment for Bayesian Inference*. R package version 16.1.4.
- Stranger, B. E., A. C. Nica, M. S. Forrest, A. Dimas, C. P. Bird, C. Beazley, C. E. Ingle, M. Dunning, P. Flicek, D. Koller, S. Montgomery, S. Tavaré, P. Deloukas, and E. T. Dermitzakis (2007). Population genomics of human gene expression. *Nature Genetics* 39(10), 1217–1224.
- Tan, L. S. L., A. Jasra, M. De Iorio, and T. M. D. Ebbels (2017). Bayesian inference for multiple Gaussian graphical models with application to metabolic association networks. *The Annals of Applied Statistics* 11(4), 2222–2251.
- Tierney, L. (1994). Markov chains for exploring posterior distributions. *The Annals of Statistics* 22(4), 1701–1762.
- Uhler, C., A. Lenkoski, and D. Richards (2018, February). Exact formulas for the normalizing constants of Wishart distributions for graphical models. *The Annals of Statistics* 46(1), 90–118.
- van den Boom, W., A. Jasra, M. D. Iorio, A. Beskos, and J. G. Eriksson (2021). Unbiased approximation of posteriors via coupled particle Markov chain Monte Carlo. arXiv:2103.05176v1.
- Vehtari, A., A. Gelman, D. Simpson, B. Carpenter, and P.-C. Bürkner (2021). Rank-normalization, folding, and localization: An improved  $\hat{R}$  for assessing convergence of MCMC. *Bayesian Analysis*. Advance online publication.

- Wang, H. (2010). Sparse seemingly unrelated regression modelling: Applications in finance and econometrics. *Computational Statistics & Data Analysis* 54(11), 2866–2877.
- Wang, H. (2015). Scaling it up: Stochastic search structure learning in graphical models. *Bayesian Analysis* 10(2), 351–377.
- Wang, H. and C. M. Carvalho (2010). Simulation of hyper-inverse Wishart distributions for non-decomposable graphs. *Electronic Journal of Statistics* 4, 1470–1475.
- Wang, H. and S. Z. Li (2012). Efficient Gaussian graphical model determination under G-Wishart prior distributions. *Electronic Journal of Statistics* 6, 168–198.
- Zanella, G. (2019). Informed proposals for local MCMC in discrete spaces. *Journal of the American Statistical Association* 115(530), 852–865.
- Zhou, S., P. Rütimann, M. Xu, and P. Bühlmann (2011). High-dimensional covariance estimation based on Gaussian graphical models. *The Journal of Machine Learning Research* 12, 2975–3026.

## A Derivation of Equation (6)

By Equation (20) of Roverato (2002),

$$p(\Phi^e \mid G, Y) \propto \exp \left[ -\frac{1}{2} \text{tr} \{ (\Phi^e)^\top \Phi^e D^{*,e} \} \right] \prod_{i=1}^p (\Phi_{ii}^e)^{\delta^* + \nu_i^{G^e} - 1} \text{ where}$$

$\nu_i^{G^e} = |\{j \mid (i, j) \in E^e \text{ and } i < j\}|$ . This density factorises as

$$p(\Phi^e \mid G, Y) \propto f(\Phi^e) \exp \left\{ -\frac{1}{2} (\Phi_{pp}^e)^2 D_{pp}^{*,e} \right\} (\Phi_{pp}^e)^{\delta^* - 1} \text{ where } f(\Phi^e) \text{ is constant with respect to}$$

$\Phi_{pp}^e$ . Thus,  $p(\Phi_{pp}^e \mid G, \Phi_{p-1,p}^e, \Phi_{-f}^e, Y) \propto \exp \left\{ -\frac{1}{2} (\Phi_{pp}^e)^2 D_{pp}^{*,e} \right\} (\Phi_{pp}^e)^{\delta^* - 1}$ . The transformation of variables  $\Phi_{pp}^e \rightarrow (\Phi_{pp}^e)^2$  yields

$$p\{(\Phi_{pp}^e)^2 \mid G, \Phi_{p-1,p}^e, \Phi_{-f}^e, Y\} \propto \exp \left\{ -\frac{1}{2} (\Phi_{pp}^e)^2 D_{pp}^{*,e} \right\} \{(\Phi_{pp}^e)^2\}^{\delta^*/2 - 1} \text{ from which Equation (6)}$$

follows.

## B Derivation of WWA's Acceptance Probabilities

This appendix derives in detail the acceptance ratios  $\widehat{R}_{\text{DA}}$  and  $R_{\text{DA}}$  used in Algorithm 2. The informed proposal  $Q(\widetilde{G} \mid G, K)$  depends on the value of  $\Phi_{p-1,p}^e$ . Thus, we need to treat the single edge update as a joint update of  $\Phi_{p-1,p}^e$  and  $G$  to derive its acceptance probability. The update is transdimensional since  $\Phi_{p-1,p}^e$  is fixed or free depending on  $G$  per (5). We therefore consider reversible jump MCMC (Green, 1995) for this derivation. Ultimately, the exchange algorithm (Murray et al., 2006), used to avoid intractable normalisation constants, circumvents the need for a reversible jump as exchanging variables does not affect their joint dimensionality, but the intermediate reversible jump acceptance probability is used to derive the approximate acceptance ratio  $\widehat{R}_{\text{DA}}$  for use with delayed acceptance MCMC.

### B.1 Reversible Jump

Recall  $\Phi_{-f}^e = \Phi^e \setminus \{\Phi_{p-1,p}^e, \Phi_{pp}^e\}$ . By construction,  $\widetilde{\Phi}_{-f}^e = \Phi_{-f}^e$ . WWA uses the joint proposal

$$q(\widetilde{G}, \widetilde{\Phi}_{p-1,p}^e \mid G, K) = Q(\widetilde{G} \mid G, K) q(\widetilde{\Phi}_{p-1,p}^e \mid \widetilde{G}, \Phi_{-f}^e)$$

Algorithm 2 chooses  $q(\widetilde{\Phi}_{p-1,p}^e \mid \widetilde{G}, \Phi_{-f}^e) = p(\widetilde{\Phi}_{p-1,p}^e \mid \widetilde{G}, \widetilde{\Phi}_{-f}^e, Y)$  given by (5) which is thus a Dirac delta function if  $e \notin \widetilde{G}$ . Therefore, the previous display reduces to

$$q(\widetilde{G}, \widetilde{\Phi}_{p-1,p}^e \mid G, K) = \begin{cases} Q(\widetilde{G} \mid G, K), & \widetilde{\Phi}_{p-1,p}^e = \phi^e \text{ and } e \notin \widetilde{E}, \\ p(\widetilde{\Phi}_{p-1,p}^e \mid \widetilde{G}, \widetilde{\Phi}_{-f}^e, Y) Q(\widetilde{G} \mid G, K), & e \in \widetilde{E}, \end{cases} \quad (14)$$

where  $\phi^e$  equals the right-hand side of (5b),  $Q(\widetilde{G} \mid G, K)$  is a probability mass function and  $p(\widetilde{\Phi}_{p-1,p}^e \mid \widetilde{G}, \widetilde{\Phi}_{-f}^e, Y)$  is a density with respect to Lebesgue measure.

The target distribution is

$$p(G, \Phi_{p-1,p}^e \mid \Phi_{-f}^e, Y) = \begin{cases} p(G \mid \Phi_{-f}^e, Y), & \Phi_{p-1,p}^e = \phi^e \text{ and } e \notin E, \\ p(\Phi_{p-1,p}^e \mid G, \Phi_{-f}^e, Y) p(G \mid \Phi_{-f}^e, Y), & e \in E. \end{cases} \quad (15)$$

This target, including  $\Phi_{p-1,p}^e$  and  $\Phi_{-f}^e$ , depends on  $e$  and thus on the proposed  $\widetilde{G}$ . Such dependence on the proposed graph does not affect the MCMC's validity or the acceptance

probability as the resulting Markov kernel can be interpreted as a mixture of kernels which each have  $p(G, K | Y)$  as invariant distribution (Tierney, 1994, Section 2.4).

Reversible jump involves a dimension-matching map. In our setting, we consider the mapping  $(\Phi_{p-1,p}^e, \tilde{\Phi}_{p-1,p}^e) \rightarrow (\tilde{\Phi}_{p-1,p}^e, \Phi_{p-1,p}^e)$  which has matched dimensions since both sides contain exactly one free element. Moreover, the absolute value of the determinant of the Jacobian of this map equals one. Therefore, the acceptance probability follows as  $1 \wedge R_{\text{RJ}}$  where (Green, 1995, Equation (7))

$$R_{\text{RJ}} = \frac{p(\tilde{G}, \tilde{\Phi}_{p-1,p}^e | \tilde{\Phi}_{-f}^e, Y) q(G, \Phi_{p-1,p}^e | \tilde{G}, \tilde{K})}{p(G, \Phi_{p-1,p}^e | \Phi_{-f}^e, Y) q(\tilde{G}, \tilde{\Phi}_{p-1,p}^e | G, K)}. \quad (16)$$

Bayes' rule and  $\tilde{\Phi}_{-f}^e = \Phi_{-f}^e$  yields

$$\frac{p(\tilde{G} | \tilde{\Phi}_{-f}^e, Y)}{p(G | \Phi_{-f}^e, Y)} = \frac{p(Y, \tilde{G}, \tilde{\Phi}_{-f}^e)}{p(Y, G, \Phi_{-f}^e)} = \frac{p(Y, \tilde{\Phi}_{-f}^e | \tilde{G}) p(\tilde{G})}{p(Y, \Phi_{-f}^e | G) p(G)}.$$

Combining the last two displays, and inserting Equations (14) and (15) provide

$$\begin{aligned} R_{\text{RJ}} &= \frac{p(\tilde{G}, \Phi_{-f}^e | Y) Q(G | \tilde{G}, \tilde{K})}{p(G, \Phi_{-f}^e | Y) Q(\tilde{G} | G, K)} = \frac{p(Y, \Phi_{-f}^e | \tilde{G}) p(\tilde{G}) Q(G | \tilde{G}, \tilde{K})}{p(Y, \Phi_{-f}^e | G) p(G) Q(\tilde{G} | G, K)} \\ &= N(\Phi_{-f}^e, D^{*,e})^{|\tilde{E}|-|E|} \frac{p(\tilde{G}) I_G(\delta, D) Q(G | \tilde{G}, \tilde{K})}{p(G) I_{\tilde{G}}(\delta, D) Q(\tilde{G} | G, K)}, \end{aligned} \quad (17)$$

where the last equality follows from Equation (1).

## B.2 Exchange Algorithm

Equation (17) cannot be used directly as it contains the intractable  $I_G(\delta, D)$ . Using the exchange algorithm avoids evaluating this normalisation constant as in Wang and Li (2012, Section 5.2) and Cheng and Lenkoski (2012, Section 2.3) by considering an augmented target distribution.

Our augmented target is a joint distribution on  $(G, K, \tilde{G}, \tilde{\Phi}_{-f}^{0,e})$  that mimics Algorithm 2. Specifically,  $(G, K)$  follows the unaugmented target distribution  $p(G, K | Y)$ , the distribution of  $\tilde{G} | G, K$  is the informed proposal  $Q(\tilde{G} | G, K)$ , and the distribution of  $\tilde{\Phi}_{-f}^{0,e} | G, K, \tilde{G}$  follows from the node reordering resulting from the pair  $(G, \tilde{G}), \tilde{K}^{0,e} | \tilde{G} \sim \mathcal{W}_{\tilde{G}^e}(\delta, D^e)$  and

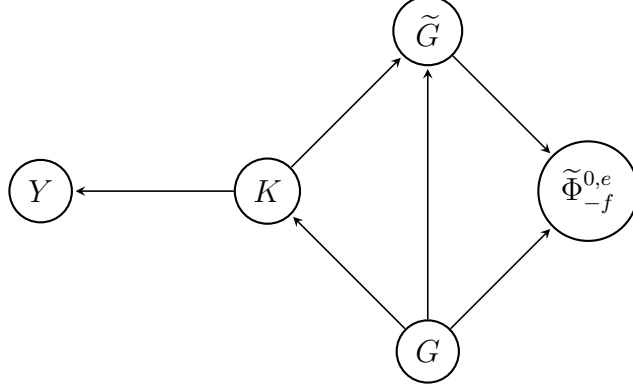


Figure 4: A directed acyclic graph representing the conditional dependence structure of the augmented target distribution (18) used with the exchange algorithm.

the definition  $\tilde{\Phi}_{-f}^{0,e} = \tilde{\Phi}^{0,e} \setminus \{\tilde{\Phi}_{p-1,p}^{0,e}, \tilde{\Phi}_{pp}^{0,e}\}$ . The augmented target distribution can thus be written as

$$\pi(G, K, \tilde{G}, \tilde{\Phi}_{-f}^{0,e}) = p(G, K | Y) Q(\tilde{G} | G, K) p(\tilde{\Phi}_{-f}^{0,e} | \tilde{G}). \quad (18)$$

Figure 4 clarifies the structure of the augmented target.

The proposal is to exchange  $G$  with  $\tilde{G}$  and update  $K$  by a value sampled from its proposal  $q(\tilde{K} | G, K, \tilde{G})$ , which is defined by sampling  $\tilde{\Phi}_{p-1,p}^e$  according to (5) while leaving the other elements of  $\tilde{\Phi}^e$  equal to the corresponding elements in  $\Phi^e$ . The resulting Metropolis-Hastings step has the posterior of interest  $p(G, K | Y)$  as target marginally on  $(G, K)$ . The remainder of this section evaluates the corresponding acceptance probability  $1 \wedge R_{\text{exchange}}^{\text{informed}}$  with

$$\begin{aligned} R_{\text{exchange}}^{\text{informed}} &= \frac{\pi(\tilde{G}, \tilde{K}, G, \tilde{\Phi}_{-f}^{0,e}) q(K | \tilde{G}, \tilde{K}, G)}{\pi(G, K, \tilde{G}, \tilde{\Phi}_{-f}^{0,e}) q(\tilde{K} | G, K, \tilde{G})} \\ &= \frac{p(\tilde{G}, \tilde{K} | Y) Q(G | \tilde{G}, \tilde{K}) p(\tilde{\Phi}_{-f}^{0,e} | G) q(K | \tilde{G}, \tilde{K}, G)}{p(G, K | Y) Q(\tilde{G} | G, K) p(\tilde{\Phi}_{-f}^{0,e} | \tilde{G}) q(\tilde{K} | G, K, \tilde{G})} \end{aligned} \quad (19)$$

where the last equality follows from (18).

The distribution  $q(\tilde{K} | G, K, \tilde{G})$  is defined through  $\tilde{\Phi}_{p-1,p}^e$  being distributed according to (5). The implied distribution on  $\tilde{K}$  follows from the transformation  $\tilde{\Phi}^e \rightarrow \tilde{K}$  such that

$$q(\tilde{K} | G, K, \tilde{G}) = J(\tilde{\Phi}^e \rightarrow \tilde{K}) q(\tilde{\Phi}_{p-1,p}^e | \tilde{G}, \Phi_{-f}^e)$$

where  $J(\tilde{\Phi}^e \rightarrow \tilde{K})$  is the Jacobian term resulting from the transformation of variables.

Similarly,

$$p(G, K | Y) = J(\Phi^e \rightarrow K) p(G, \Phi^e | Y).$$

These Jacobian terms cancel in  $R_{\text{exchange}}^{\text{informed}}$ . Specifically, inserting the previous two displays into (19) yields

$$R_{\text{exchange}}^{\text{informed}} = \frac{p(\tilde{G}, \tilde{\Phi}^e | Y) Q(G | \tilde{G}, \tilde{K}) p(\tilde{\Phi}_{-f}^{0,e} | G) q(\Phi_{p-1,p}^e | G, \tilde{\Phi}_{-f}^e)}{p(G, \Phi^e | Y) Q(\tilde{G} | G, K) p(\tilde{\Phi}_{-f}^{0,e} | \tilde{G}) q(\tilde{\Phi}_{p-1,p}^e | \tilde{G}, \Phi_{-f}^e)}.$$

Consider the factorisation  $p(G, \Phi^e | Y) = p(G, \Phi_{p-1,p}^e | \Phi_{pp}^e, \Phi_{-f}^e, Y) p(\Phi_{pp}^e, \Phi_{-f}^e | Y)$ . The proposal is such that  $\tilde{\Phi}_{pp}^e = \Phi_{pp}^e$  and  $\tilde{\Phi}_{-f}^e = \Phi_{-f}^e$ . We also make use of the equality  $p(G, \Phi_{p-1,p}^e | \Phi_{pp}^e, \Phi_{-f}^e, Y) = p(G, \Phi_{p-1,p}^e | \Phi_{-f}^e, Y)$  since  $\Phi_{pp}^e$  is independent of  $(G, \Phi_{-f}^e, \Phi_{p-1,p}^e)$  by (6). Thus,

$$\frac{p(\tilde{G}, \tilde{\Phi}^e | Y)}{p(G, \Phi^e | Y)} = \frac{p(\tilde{G}, \tilde{\Phi}_{p-1,p}^e | \tilde{\Phi}_{pp}^e, \tilde{\Phi}_{-f}^e, Y) p(\tilde{\Phi}_{pp}^e, \tilde{\Phi}_{-f}^e | Y)}{p(G, \Phi_{p-1,p}^e | \Phi_{pp}^e, \Phi_{-f}^e, Y) p(\Phi_{pp}^e, \Phi_{-f}^e | Y)} = \frac{p(\tilde{G}, \tilde{\Phi}_{p-1,p}^e | \tilde{\Phi}_{-f}^e, Y)}{p(G, \Phi_{p-1,p}^e | \Phi_{-f}^e, Y)}.$$

Furthermore,  $Q(\tilde{G} | G, K) q(\tilde{\Phi}_{p-1,p}^e | \tilde{G}, \Phi_{-f}^e) = q(\tilde{G}, \tilde{\Phi}_{p-1,p}^e | G, K)$  where  $q(\tilde{G}, \tilde{\Phi}_{p-1,p}^e | G, K)$  is given by (14). Combined with the previous two displays, we obtain

$$\begin{aligned} R_{\text{exchange}}^{\text{informed}} &= \frac{p(\tilde{G}, \tilde{\Phi}_{p-1,p}^e | \tilde{\Phi}_{-f}^e, Y) q(G, \Phi_{p-1,p}^e | \tilde{G}, \tilde{K}) p(\tilde{\Phi}_{-f}^{0,e} | G)}{p(G, \Phi_{p-1,p}^e | \Phi_{-f}^e, Y) q(\tilde{G}, \tilde{\Phi}_{p-1,p}^e | G, K) p(\tilde{\Phi}_{-f}^{0,e} | \tilde{G})} \\ &= R_{\text{RJ}} \frac{p(\tilde{\Phi}_{-f}^{0,e} | G)}{p(\tilde{\Phi}_{-f}^{0,e} | \tilde{G})} \end{aligned}$$

where the last equality follows from (16). Inserting (17) and recalling (4) yields

$$R_{\text{exchange}}^{\text{informed}} = R_{\text{exchange}} \frac{Q(G | \tilde{G}, \tilde{K})}{Q(\tilde{G} | G, K)}.$$

The acceptance probabilities in Algorithm 2 follow now from the delayed acceptance method in Algorithm 1 of Christen and Fox (2005). Specifically,  $\hat{R}_{\text{DA}}$  equals  $R_{\text{RJ}}$  with the ratio of normalising constants in (17) approximated by (7). Then, the second accept-reject step uses  $R_{\text{exchange}}$  from Equation (4) in place of the ratio of target distributions like  $R_{\text{exchange}}^{\text{informed}}$  does.

## C Algorithm from Cheng and Lenkoski (2012)

We describe the CL algorithm of Cheng and Lenkoski (2012) in Algorithm 3 to aid the discussion in Section 2.6. To highlight connections with WWA, we use the delayed acceptance

framework to describe the algorithm even though Cheng and Lenkoski (2012) do not use such terminology.

The first accept-reject step in Step 1c of Algorithm 3 uses  $\widehat{R}_{\text{CL}}$  as odds instead of acceptance ratio. This provides a correspondence with Barker's algorithm (Barker, 1965): write  $\widehat{R}_{\text{CL}} = \tilde{z}/z$  for some positive numbers  $z$  and  $\tilde{z}$  that correspond with the current and proposed state, respectively. Denote the acceptance probability by  $\alpha$ . Accepting with odds  $\widehat{R}_{\text{CL}}$  means  $\widehat{R}_{\text{CL}} = \alpha/(1 - \alpha)$ . Then,  $\alpha = \tilde{z}/(z + \tilde{z})$  which is Barker's acceptance probability. Using  $\widehat{R}_{\text{CL}}$  as acceptance ratio would yield the Metropolis-Hastings acceptance probability  $\alpha = 1 \wedge \widehat{R}_{\text{CL}}$ .

---

**Algorithm 3** (Cheng and Lenkoski, 2012) A Single MCMC Step of the CL Algorithm.

---

**Input:** Precision matrix  $K$  and graph  $G$ .

**Output:** MCMC update for  $(G, K)$  such that the invariant distribution is approximately the posterior  $p(G, K | Y)$ .

1. For each edge  $e \in \{(i, j) \mid 1 \leq i < j \leq p\}$ , do the following:

- (a) Let  $\tilde{G} = (V, \tilde{E})$  where  $\tilde{E} = E \cup \{e\}$  if  $e \notin E$  and  $\tilde{E} = E \setminus \{e\}$  otherwise.
- (b) Reorder the nodes in  $G$  and  $\tilde{G}$  so that  $e$  connects node  $p-1$  and  $p$ . Rearrange  $D$ ,  $D^*$  and  $K$  accordingly. Denote the resulting quantities with a superscript  $e$ .
- (c) Denote the upper triangular Cholesky decomposition of  $K^e$  by  $\Phi^e$ . ‘Promote’  $\tilde{G}$  to be considered for delayed acceptance with odds  $\hat{R}_{\text{CL}}$  where

$$\hat{R}_{\text{CL}} = \frac{p(\tilde{G})}{p(G)} N(\Phi_{-f}^e, D^{*,e})^{|\tilde{E}| - |E|}$$

with  $N(\Phi_{-f}^e, D^{*,e})$  given by Equation (2). If  $\tilde{G}$  is promoted:

- i. Generate a  $\tilde{K}^{0,e}$  by running the block Gibbs sampler from Wang and Li (2012) initialised at  $K^e$  and with  $\mathcal{W}_{\tilde{G}^e}(\delta, D^e)$  as stationary distribution.
- ii. Compute the upper triangular Cholesky decomposition  $\tilde{\Phi}^{0,e}$  of  $\tilde{K}^{0,e}$ .
- iii. Set  $G = \tilde{G}$  and  $K = \tilde{K}$  w.p.  $1 \wedge N(\tilde{\Phi}_{-f}^{0,e}, D^e)^{|E| - |\tilde{E}|}$ .
- (d) Update  $K$  by resampling  $\Phi_{p-1,p}^e$  and  $\Phi_{pp}^e$  according to  $G^e$ .

2. Resample  $K$  by running the block Gibbs sampler from Wang and Li (2012) with  $\mathcal{W}_G(\delta^*, D^*)$  as stationary distribution.

---